Interferences in Safety Critical Land Transport Application: Notch Filtering vs Wavelet Transform, an Experimental Analysis

Syed Ali Kazim, Juliette Marais, Nourdine Ait Tmazirte

Interferences in Safety Critical Land Transport Application: Notch Filtering vs Wavelet Transform, an Experimental Analysis

Kazim S.Ali, Marais. J, Aït Tmazirte, N.
COSYS-LEOST, Univ Gustave Eiffel, Univ Lille,
Villeneuve d'Ascq, FRANCE

Biography(ies)

Syed Ali Kazim has a master's degree in Electronic Engineering and later he completed a specialization degree in Navigation and Related Applications from Politecnico di Torino (Italy) in 2017. He is currently a Ph.D. student at University Gustave Eiffel. His research activities are mainly devoted to GNSS signal characterization, error modeling and localization systems.

Nourdine Aït Tmazirte is a research engineer at University Gustave Eiffel since 2021. He got his engineering and M.Sc. degree in automation engineering from Ecole Centrale de Lille, France, both in 2010. His research interests include multi-sensor fault-tolerant fusion for localization and integrity assessment.

Dr. Juliette Marais received an engineering degree from Institut Supérieur de l'Electronique et du Numérique. She received a Ph.D. degree in electronics and the "Habilitation à diriger des recherches" from the University of Lille, France, in 2002 and 2017 respectively. Since 2002, she has been a research fellow with Université Gustave Eiffel (former IFSTTAR). Her research interest is in GNSS performance analysis and enhancement considering the specificity of propagation effects in transport harsh environments. Her research interests principally include local propagation phenomena, positioning and pseudorange error modelling, detection and mitigation of local effects for better accuracy and integrity with some contributions to EU and national projects.

Abstract

In safety-critical applications, the vulnerability of the Global Navigation Satellite System (GNSS) to radio frequency interferences (RFIs) is a major concern. The development of a fail-safe and robust localization system now necessarily requires detection and mitigation of such interferences, which has increased with the proliferation of wireless systems and easy access to personal privacy devices (PPD) also known as jammers. Moreover, the advent of software-defined radio (SDR) permitting the transmission of customized and more complex signals has further complicated this problem. This paper provides an in-depth comparison of interference mitigation techniques at multiple levels primarily focusing on the safety perspective at the position level. For this purpose, the classical adaptive notch filter (ANF) and the wavelet packet decomposition method are applied to mitigate the effects of interference. This comparative study aims to assess the performance of these mitigation techniques at multiple levels (frequency estimation, acquisition, tracking and position). However, the main goal for the final user is to study the impact on key performance indicators (KPIs) such as accuracy, availability, and safety. Furthermore, two cases are considered: 1): interference in the absence of any mitigation strategy and after applying interference mitigation technique at the pre-correlation level. The complete study is presented for two different types of time-varying continuous wave (CW) interference signals namely frequency hopping and the chirp signal.

1. INTRODUCTION

The localization function designed for terrestrial applications inherits high-level performance requirements to guarantee accuracy, availability, continuity and operation safety. These requirements are perceived to be much more stringent for forthcoming generation as it aims to bring more intelligence, autonomy, connectivity and shared mobility services. It necessitates reliable positioning and navigation among other key requirements to accomplish some of these goals. It implies considering and managing all the risks and threats associated with a positioning system to ensure a fail-safe positioning solution, particularly in the case of satellite-based positioning systems.
Global Navigation Satellite System (GNSS) is recognized as a Game Changer technology for many applications that can bring economic and ecological incentives, particularly in the railway sector for signaling applications. However, its performance is mainly associated to receiver operating conditions. This makes it very challenging for a satellite-

based positioning system to meet performance requirements as the satellite signals are vulnerable to obstacles present around the receiver. It is particularly prone to unintended and malicious radio transmissions from jammers.
There exist several approaches for the detection and mitigation of interference signals which are mainly implemented at the Front-end, pre-correlation, post-correlation, and navigation levels in the receiver chain (Dovis, 2015). It includes signal processing techniques (Anyaegbu et al., 2008; Borio, 2016; Borio, et al., 2008; Borio & Cano, 2013; Dovis et al., 2012) to filter the interference signal that filters IQ samples either in time, frequency, or time-frequency/scale domain; Spatial filtering (Fu et al., 2003; Gupta & Moore, 2003) which requires processing signals acquired from several antennas mounted in an array. This permits to digitally steer the beam pattern in the direction of the satellite signals while suppressing the unwanted signal from the interference source; Vector tracking (Lashley et al., 2009; Nunes et al., 2010) allows to track the satellite signal in cooperation with other satellite channels. In this manner, it enhances the tracking capability of largely degraded signals consequently increasing the overall performance. Sensor fusion (Groves & Long, 2005) makes use of the information from the inertial sensors to counter the impact of interference.
In this study, we are interested in the detection and mitigation of interference signals at the pre-correlation level. The primary goal is to evaluate performance from the user's perspective. Several countermeasures at the pre-correlation level show high performance in mitigating the effect of an interfering signal. However, their performance is assessed mainly at the signal level (at either acquisition or tracking stage). Recently, some studies presented the impact of interference and mitigation techniques effectiveness at the position level (Borio & Gioia, 2021; Gioia & Borio, 2021). Similarly, we also addressed interference mitigation from a safety perspective (Kazim et al., 2021). We provided KPIs assessment in the presence of interfering signal and after enabling mitigation block implemented within the receiver. This study is the extension of our previous work where we now have implemented two interference mitigation techniques namely adaptive notch filter (ANF) and wavelet packet decomposition (WPD) to counter the interference signal. For each technique, it presents an in-depth discussion and a comparative analysis at multiple levels (frequency estimation, acquisition, tracking, and position). Furthermore, it also provides an assessment at the positioning level discussing previously mentioned KPIs using the Stanford representation. This study provides a performance assessment for two different types of time-varying CW interference signals namely frequency hopping and chirp signal
The paper is organized into several sections. Section 2 provides some details on the state of the art interference mitigation techniques namely Adaptive Notch Filter (ANF) and Wavelet Packet Decomposition (WPD). Section 3 provides an overview of the used positioning algorithm based on the weighted least square (WLS) solution. Three well-known weighting schemes based on elevation, carrier to noise ratio (C/N_0) and a hybrid model are briefly presented. Moreover, it also presents a classical manner to estimate the protection level using Hslope estimation. Section 4 describes the experimental setup used for data recording and it also provides details on the interference scenarios and acquisition campaigns performed during the day at regular intervals. Finally, a performance assessment based on the experimental results for the two cases: interference without any mitigation and after applying interference countermeasures for the chirp and frequency-hopping scenario is presented before discussion.

2. INTERFERENCE SUPPRESSION AT THE PRECORRELATION STAGE

In literature, the issue of radio frequency interference is largely investigated at the pre-correlation level. Several techniques have been proposed for the detection, characterization, mitigation and in some cases localization of the interference source. The most common mitigation method includes Pulse Blanking (PB), Adaptive Notch Filter (ANF), Short Time Fourier Transform (STFT), Wigner-Ville Distribution (WVD), Wavelet Transform (WT), and Kerhunen-Loève Transform (KLT). In general, each technique aims to estimate the interference components and subsequently applies a mitigation process for the suppression. In this work, Adaptive Notch Filter (ANF) and Wavelet Packet Decomposition (WPD) have been investigated as interference mitigation techniques. This section will provide a brief overview of the two considered mitigation techniques.

1. Adaptive Notch Filter (ANF)

An Adaptive Notch Filter (ANF) is a widely used method for the suppression of narrowband interference signals. It is comprised of a notch filter to reject a very narrow portion of the signal and an adaptive unit to continuously estimate the instantaneous frequency of the jamming signal. Thus, in this manner, it effectively tracks and suppresses the interfering signal without affecting much of the useful component of the signal. The transfer function of the single-pole Infinite Impulse Response (IIR) notch filter is given as:

$$H(z) = \frac{1 - z_0 z^{-1}}{1 - k_\alpha z_0 z^{-1}} \quad (1)$$

where $k_\alpha \epsilon [0,1)$ represents the pole contraction that controls the bandwidth of the notch, z_0 represents filter zero in the complex plane which in the lock state corresponds to the interference frequency. The transfer function of the filter can be split into the moving average (MA) and autoregressive (AR) blocks. The output from each block can be expressed as

$$x_r[n] = x[n] + k_\alpha z_0 x_r[n-1] \quad (2)$$

$$y_m[n] = x[n] - z_0 x_r[n-1] \quad (3)$$

Where $x_r[n]$ and $y_m[n]$ represents the output from the AR and the MA function respectively. Ideally, a very narrow rejection bandwidth allows the filter to largely suppress interference frequency while preserving mostly useful content of the signal. This condition is obtained when the notch frequency is equivalent to the interference instantaneous frequency. The 3dB bandwidth of the filter can be estimated as:

$$B_{3dB} \approx (1 - k_\alpha) f_s \pi / 10 \quad (4)$$

where a narrow notch is achieved as the value of k_α approaches to unity ($k_\alpha \to 1$). The function of the adaptive block is to move filter zero z_0 progressively in a complex plane until it converges to interference frequency. It is based on the iterative normalized least mean square (LMS) algorithm, which minimizes the cost function. It could be estimated either by minimizing the expectation of the filter output energy or by minimizing the expectation of MA output energy. The minimization is achieved from the filter output through an iterative rule to estimate filter zero z_0 in the runtime.

$$z_0[n] = z_0[n-1] - \mu[n] g(J[n]) \quad (5)$$

where $\mu[n] = \frac{\delta}{E\{|x_r[n]|^2\}}$ is the algorithm step, $E\{|x_r[n]|^2\}$ is the power of AR block output, δ is an unnormalized LMS algorithm step that controls the convergence properties of the algorithm, $g(J[n])$ is the stochastic gradient of the cost function $J[n]$.

$$g(J[n]) = y_m[n] x_r^*[n-1] \quad (6)$$

An adaptive notch filter serves as a very simple but very effective technique to suppress interference, particularly for chirp signals. However, its performance depends on the appropriate selection of the filter parameters (Qin et al., 2020). The two important parameters are notch width k_α and algorithm step δ which must be tuned properly to achieve better performance. Furthermore, the main drawback of ANF is that it is not a very effective method for dealing with multiple interfering signals simultaneously present in the GNSS band. (Landry et al., 1998) presented an all-pass filter with a Gauss-Newton algorithm as an adaptive algorithm to enhance the convergence rate to suppress CWI and swept CW interference. (Borio, Camoriano, & Presti, 2008) presented multi-pole adaptive filter by cascading several two-pole IIR notch filters to progressively blocks multiple CW interfering signals.

2. Discrete Wavelet Transform (DWT)

Wavelet analysis is well-known among the families of transformation techniques used to characterize the signal components. In wavelet transform, a discrete signal is decomposed using a set of orthogonal functions which are derived by scaling and shifting the mother wavelet function. In this manner, it uses a scalable window to transform a time domain signal into a time-scale (frequency) domain. Thus, it overcomes the shortcoming of fixed time window operation as in the case of Short Time Fourier Transform (STFT).

In Discrete Wavelet Transform (DWT), the decomposition stages are mainly realized by bandpass filtering and subsampling process. The signal is passed through a bank of wavelet-based bandpass filters with different cut-off frequencies at different scales. The filtering operation splits the incoming signal into low and high frequency bands at

each decomposition stage. The low pass filter, equivalent to averaging operation extracts the coarse approximation whereas the highpass filter similar to differencing operation acquires the detailed information of the signal. Later, a decimation process equivalent to a downsampling operation is performed to reduce sample redundancy induced by the filtering process. It is accomplished by eliminating every alternative sample to remain in compliance with Nyquist's sampling criterion. The same procedure is repeated at each level until the desired decomposition level is reached. Consequently, at every decomposition stage, the time resolution is reduced by the factor of ½ (half of the samples describe the decomposed signal) gaining twice in the frequency resolution. This reduces the uncertainty in the frequency as the signal splits into low and high frequency bands. The decomposition stages of a discrete signal $x(k)$ for different bands at different scales is shown in Figure 1.

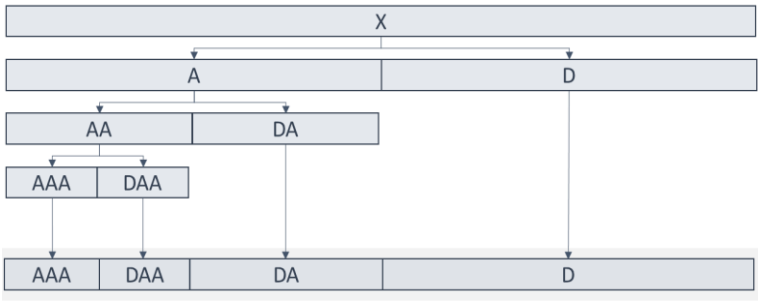

Figure 1 *An Illustration of 3-Level Discrete Wavelet Decomposition (DWT); Approximation (A) And Detail (D) Block Represent the Low Pass and High Pass Filtering and The Subsampling Operation*

The decomposition level can be mathematically expressed as:

$$y_{low}[n] = \sum_{k=-\infty}^{\infty} x[k]g[2n-k] \tag{7}$$

$$y_{high}[n] = \sum_{k=-\infty}^{\infty} x[k]h[2n-k] \tag{8}$$

where y_{low} and y_{high} represent the decomposed signal output from the low pass and high pass filters respectively and after performing downsampling by factor 2. The scaling vector $g[n]$ and wavelet vector $h[n]$ represent impulse response of low pass and high pass filter respectively.

Discrete Wavelet Transform (DWT) can be further extended to form a decomposition tree also known as Wavelet Packet Decomposition (WPD). The two methods differ in the sense that, in WPD, the detailed branch (high frequency

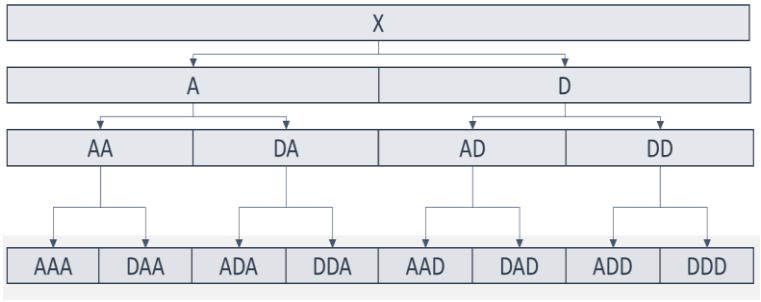

Figure 2 *An Illustration of 3-Level Discrete Wavelet Packet Decomposition (WPD); Approximation (A) And Detail (D) Block Represent Low Pass and High Pass Filtering Respectively, and Subsampling Operation.*

band) is also decomposed similarly to the approximation branch (low frequency band) to form a tree-like structure. This process generates several additional wavelet packets after passing a signal through a uniform wavelet filter bank.

Each decomposition stage forms 2^N wavelet packets representing some portions of the input signal where N represents the decomposition level. A three-level wavelet decomposition packet using uniform filter banks is shown in Figure 2.

The main purpose of applying signal decomposition is to break down the incoming signal to get a representation where interference content can be easily identified and isolated from the useful signal. Therefore, the interference mitigation process further requires detection, mitigation and reconstruction steps.

The detection phase, at first, requires calibration of each wavelet packet in the absence of interference. In this way, a threshold is approximated in a statistical manner represented by variations in the standard deviation in time-scale representation. An interference signal is considered to be present whenever the wavelet coefficients surpass the set threshold value previously defined in the calibration phase.

In the mitigation phase, all the wavelet coefficients that exceed the set threshold defined during the calibration process (in the absence of interference) are given a null value also known as coefficient blanking. Thus, the blanking method allows the removal of extra energy which is due to the presence of an interference signal.

In the reconstruction step, the signal is reconstructed using the inverse wavelet transform. This is done using the reconstruction filters and upsampling operation while back tracing all the steps done in the decomposition process.

The performance of wavelet techniques is well assessed in the presence of CW and pulse interference signals. In (Anyaegbu et al., 2008), Wavelet Transform is used to counter the effects of pulsed interference. (Seo et al., 2019) provided a comparative study using different wavelet filters for the removal of a narrowband signal. (Musumeci & Dovis, 2014, 2013) investigated a wavelet-based interference mitigation method for pulsed and narrowband signals and analyzed the effectiveness of mitigation in the acquisition and tracking stages. (Musumeci et al., 2016) extended further the analysis and evaluated mitigation performance at position level in the presence of a narrowband interference signal.

3. INTEGRATION ALGORITHM, WEIGHTING SCHEMES AND PROTECTION LEVEL COMPUTATION

The primary goal of this study is to analyze the performance of previously presented interference mitigation techniques from the user's point of view. For this purpose, we evaluate some important performance indicators such as availability, accuracy and safety at the position level. This section presents some details on the used positioning algorithm, weighting schemes and Horizontal Protection Level (HPL)

1. Weighted Least Square (WLS) Position Estimator

The most common method to compute the position from a set of pseudorange measurements is based on Least Square (LS) method. In LS, the user position is estimated recursively relatively to the linearization point by using pseudorange errors. The linearized pseudorange equation can be written as:

$$\delta\rho = H \times \delta X + \epsilon \tag{9}$$

where $\delta\rho$ is the difference between the actual and the predicted pseudorange estimated from the linearization point, H is the observation matrix representing satellite-receiver information, δX the error state vector, ϵ is the measurement error.
The Weighted Least Square (WLS) estimator can be expressed as:

$$\delta X = [H^T W H]^{-1} H^T W \times \delta\rho \tag{10}$$

where W is the observation weighting matrix given by

$$W = \begin{pmatrix} 1/\sigma_1^2 & \cdots & 0 \\ \vdots & \ddots & \vdots \\ 0 & \cdots & 1/\sigma_m^2 \end{pmatrix} \quad (11)$$

The measurement weights are inversely proportional to the error variance ($w_i = 1/{\sigma_i}^2$). In WLS, different weights are given to the measurements based on the measurement noise. Therefore, measurements with a small error variance carry more weight hence more confidence to contribute to the position estimation. On the other hand, measurements with large error variance would get lower weight as a result have either less or no contribution at all in the position estimation.

2. Weighting Schemes

In this discussion, we present some of the most common weighting models that include carrier to noise ratio (C/N_0), satellite elevation and a hybrid model (combination of elevation and C/N_0 model). In general, weighing models are somehow used to give confidence to the measurements.

The carrier to noise ratio (C/N_0) is a measure of the power level of the received signal relative to the noise power level per unit bandwidth. It is the key parameter that defines the quality of the signal. (Hartinger & Brunner, 1999) presented a generalized expression to estimate the variance from the C/N_0 measurements. The expression for sigma-ε is expressed as:

$$\sigma^2 = a + b.10^{-0.1 \times C/N_0} \quad (12)$$

where, a (in m^2) and b (in m^2 Hz) are the model parameter that corresponds to receiver characteristics.

Satellite elevation can also be used to evaluate the quality of the signal. The elevation model exploits the fact that low elevation satellites are subjected to more errors than high elevation satellites. The variance for the elevation-based weighting model is given as:

$$\sigma_i^2 = 1/sin(el_i)^2 \quad (12)$$

The hybrid model takes into consideration of both elevation and carrier to noise ratio to estimate the variance. A hybrid model with a *k* factor as the LOS indicator (Tay & Marais, 2013) increases the effect of deweighting when NLOS signal is detected and is given as:

$$\sigma_i^2 = k\frac{10^{\frac{-C/N_{0i}}{10}}}{sin(el_i)^2} \quad (13)$$

3. Horizontal Protection Level (HPL) Computation

The Horizontal Protection Level (HPL) is a statistical bound used to guarantee that the true position error is well confined. In general, the protection level is estimated by taking into consideration the impact of measurement errors and bias on the estimated position. Thus, it provides information to the user about confidence in the estimated position. It is mainly used to evaluate the reliability of the system. HPL can be traditionally expressed as the combination of a noise term HPL_n and a biased term HPL_b:

$$HPL = HPL_n + HPL_b \quad (14)$$

The noise term is calculated according to the error propagation as for HPL computed with SBAS data (mostly for aeronautic applications):

$$HPL_n = K(P_{md}) \times d_{major} \quad (15)$$

where K is an inflation factor that permits to meet integrity risk requirements. It is generally obtained conservatively, by selecting the 4 degrees of freedom value in the χ^2 table; d_{major} is the error uncertainty along the semi-major axis of the error ellipse.

The bias term is the most affected by the change in the weighting strategy and the term *HSlope* represents the sensitivity of HPE to the bias of i^{th} satellite.

$$HPL_b = max_i \left(HSlope_i \, . \sigma_i \right) \times p_{bias} \tag{16}$$

where the slope is given as:

$$HSlope_i = \sqrt{\frac{\left(H_{N,i}^{+}\right)^2 + \left(H_{E,i}^{+}\right)^2}{S_{ii}}} \tag{17}$$

with $H^+ = [H^T W H]^{-1} H^T W$ with indexes E and N representing the components alond the East and North axes in an ENU frame; $S = I - HH^+$; σ_i is the standard deviation of the i^{th} measurement error; $p_{bias} = \sqrt{NSSE}$ (Normalized Sum of Squared Error), p_{bias} represents the bias in the space of test statistics. Finally, HPL is expressed as (Walter & Enge, 1995):

$$HPL = K(P_{md}) \times d_{major} + max_i \left(HSlope_i \, . \sigma_i \right) \times p_{bias} \tag{18}$$

4. EXPERIMENTAL PROTOCOL

1. Data Acquisition

For this study, the Stella record and playback tool from M3Systems have been used to record raw IQ signals that use Universal Software Radio Peripheral (USRP 2954R) from National Instruments as the front end to perform initial filtering and downconversion. The recording system is connected to an antenna (Adsotech ASH11661) mounted on the rooftop of our building for relatively open-sky conditions and optimal satellite visibility. This also allows minimizing the signal disturbances induced by the presence of obstacles in the close vicinity of the antenna. As far as the jammer is concerned, we have used a customizable interference source to transmit the interference signal via USRP 2910.

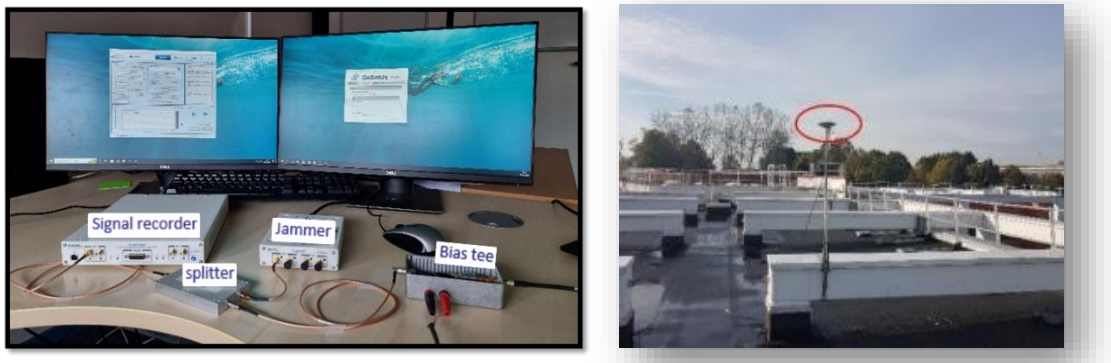

Figure 3 *GNSS Signal Recording System Connected to an Interference source (Left) and Antenna* The Roof *Mounted on The Roof of The Building to Capture Satellite Signals (Right).*

The interference and GNSS signals are then combined through a radio frequency combiner and the interfered signal is fed to the signal recorder. The complete experimental setup is shown in Figure 3. We presented two interference scenarios: 1) frequency-hopping and 2) chirp signal. This allows us to analyze the robustness of each mitigation method against two interference signals considered. The spectrogram representing the time-frequency relationship of the two interference signals is shown in Figure 4.

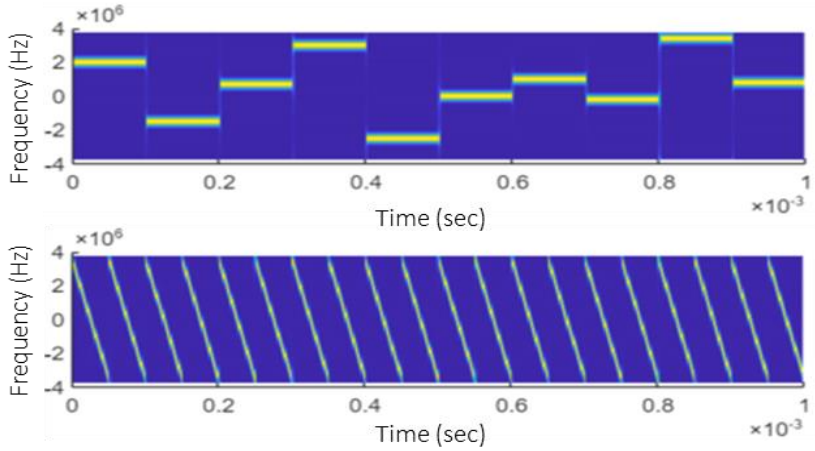

Figure 4 *Interference Scenario with Frequency Hopping (Upper Panel) And Chirp Signal (Lower Panel) At Baseband.*

Table 1 provides some details of the interference used cases and the signal recording system. In total, we have recorded 18 files (9 for each interference scenario), each of 90 seconds length. The signal acquisition has been performed during 3 different periods of the day to get different satellite configurations and visibility. The interference signal of 30-second duration is injected after 55 seconds in each recording. The recorded files are later processed individually using a Matlab-based software receiver to conduct performance analysis.

Table 1 *Receiver Configuration Used to Record GPS L1 signal with Interference signal characteristics.*

SIGNAL PARAMETERS		
RECEIVER CONFIGURATION	*central frequency*	*GPS L1 (1575.42 MHz)*
	sampling frequency	*15 MHz*
	bandwidth	*12 MHz*
	quantization	*8 bits*
FREQUENCY HOPPING	*frequency pattern*	*[2.0, -1.5, 0.7, 3, -2.5, 0.0, 1.0, -0.2, 3.4, 0.8 MHz]*
	hopping rate	*100 µsec*
	hopping period	*1 msec*
	duration	*30 sec*
CHIRP	*bandwidth*	*7 MHz*
	chirp rate	*0.14 MHz/µsec*
	sweep period	*50 µsec*
	duration	*30 sec*

The main purpose of this study is to investigate the impact of interference and the importance of mitigation from a safety perspective. Therefore, it provides performance assessment for some key positioning performance indicators such as accuracy, availability, continuity, and safety. A multi-objective comparative discussion has been made on the impact of interference and also on the performance of mitigation techniques at different stages of the receiver.

2. Results and Analysis

This section provides experimental results of a comparative performance analysis between a classical Adaptive Notch Filter (ANF) and a Wavelet Packet Decomposition (WPD) for the two considered mitigation techniques. It evaluates mitigation performance at multiple levels including interference identification and suppression and their impact on tracking and positioning level. Finally, it provides an analysis of positioning performance from the user perspectives which is not only limited to positioning accuracy but also discusses system availability and safety.

1. Identification and Mitigation of Interference

To suppress the effects of jamming, it is very important to understand the characteristics of the interfering signal. This allows selecting a countermeasure strategy in time, frequency, or time-frequency domains, where interference components can be easily identified to possibly isolate them from the useful signal. For this purpose, we applied ANF and WPD techniques to estimate the time-varying frequency of the interference signal.

Figure 5. illustrates the estimated frequency by the adaptive notch filter in the presence of frequency hopping (left) and chirp (right) signal. As previously discussed, the effectiveness of ANF-based mitigation depends on the filter parameters that require appropriate tuning depending on the characteristics of the interference signal. For simplicity, we used the same configuration ($k_\alpha = 0.8 \; and \; \delta = 0.05$) of ANF for each of the two interference scenarios. Here, ANF appears to track very closely the interference frequencies in comparison to the scenarios illustrated in Figure 4. However, in the frequency hopping scenario, the filter has shown significant oscillations around the interference frequency resulting in higher estimation noise. It is important to note that no extensive analysis is conducted on filter convergence or frequency estimation at this level.

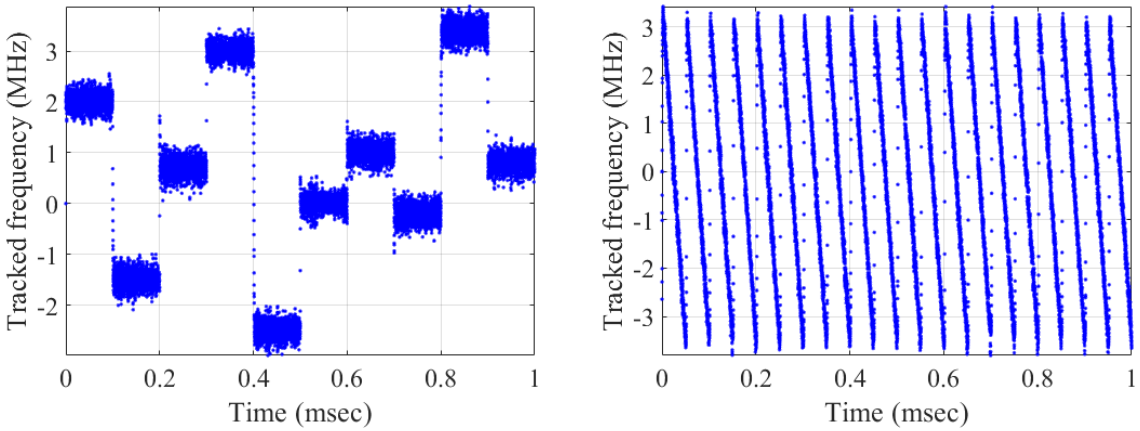

Figure 5 *Interference Frequency Tracked by Adaptive Notch Filter (Adaptation Step =0.05 and Pole Contraction Factor =0.8) In Case of Frequency Hopping (Left) and Chirp Signal (Right).*

Figure 6 illustrates a decomposed form of the interfered signal represented in the time-scale domain after applying wavelet packet decomposition (WPD). Here, a 5-level decomposition is realized using the "Symlet" function providing 32 wavelet packets, each representing some portion of signal content. The detection floor (threshold mask) is represented by the black plane which separates the clean and the interfered signal component. It is estimated by individually calibrating each wavelet packet in the nominal conditions. From the time-scale representation, it is evident that interference signal components have occupied approximately 50% of the wavelet scales which shows a high signal activity compared to higher scales. After the detection process, interference mitigation is performed in which all the coefficient values exceeding the threshold mask are set to a null value, also known as coefficient blanking. The modified wavelet packets are then fed to the synthesis filter bank to achieve signal reconstruction.

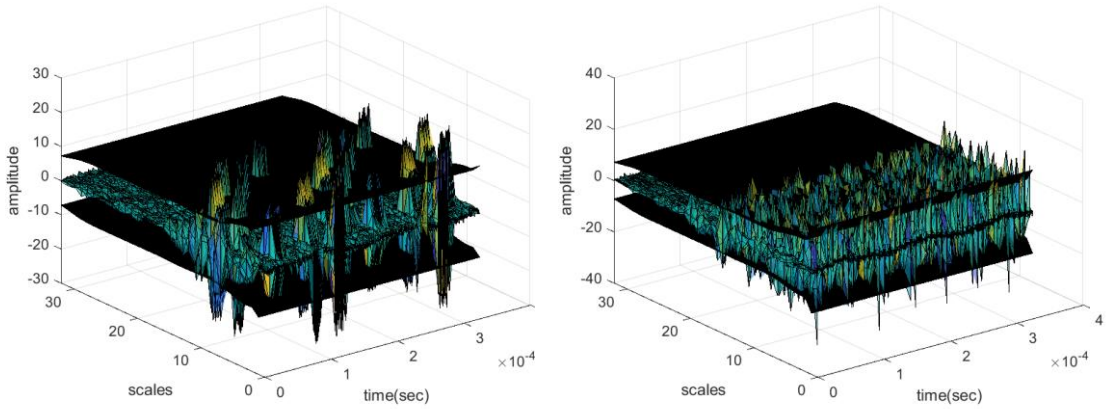

Figure 6 *Time-Scale Representation with 5 Level Decomposition of GPS L1 Signal Interfered with Frequency Hopping (Left) and Chirp Signal (Right).*

2. *Tracking*

This section aims to assess the tracking capabilities of the receiver before and after applying the mitigation techniques. Figure 7 clearly shows the impact of interference on satellite tracking in presence of frequency hopping (left) and chirp signal (right). The effects of interference can be seen approximately after 58 seconds with the emergence of the interference signal. At this point, without mitigation, the receiver completely lost track of the satellite signal (red curve). Instead, it started to track the interference signal which overpowered the satellite signal. After the removal of interference, in each mitigation scenario, the receiver started to track back the satellite signal. In the case of the chirp signal (right), the two mitigation techniques show similar performance. However, in the frequency hopping case (left), WPD-based mitigation appears to perform better with lower tracking noise compared to ANF filtering (blue).

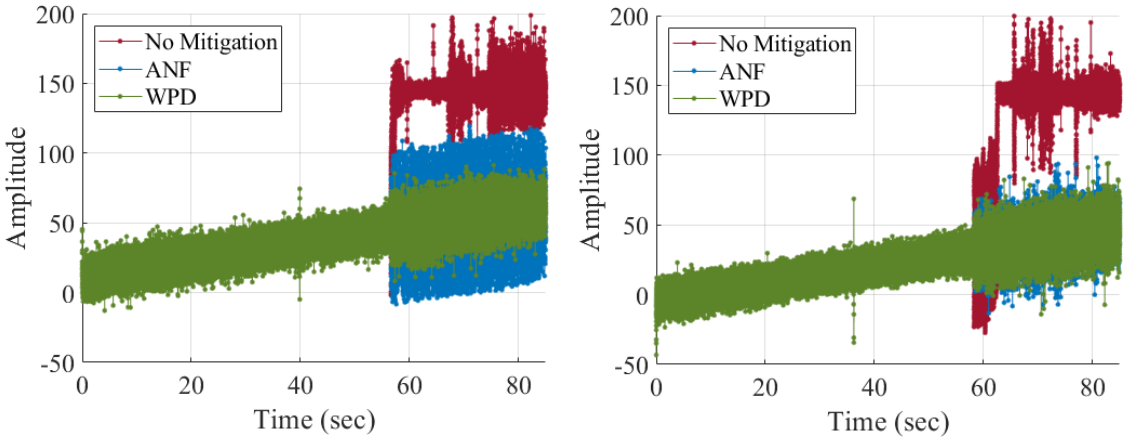

Figure 7 *Satellite (PRN 02) Tracking State in The Presence of Frequency Hopping (Left) and Chirp (Right) Interference; No Mitigation (Red), ANF (Blue) And WPD (Green).*

A similar trend appears in the carrier-to-noise ratio (C/N_0) estimation representing the tracking quality of the signal. Figure 8 shows that the C/N_0 value abnormally fluctuates in presence of an interference signal which after applying interference mitigation dropped a few dB from the nominal trend (before interference injection) due to the filtering

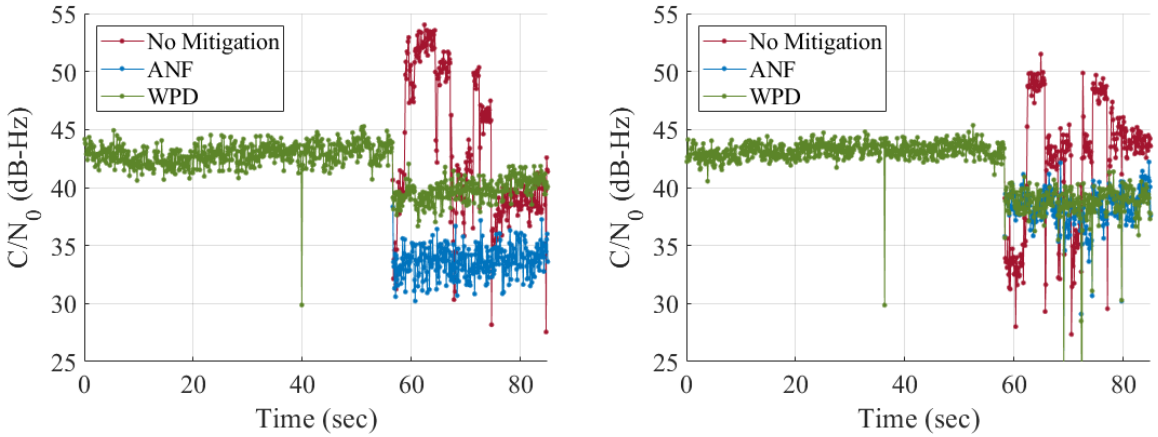

Figure 8 *Carrier to Noise Ratio (C/N_0) Estimated After Satellite Tracking Stage for PRN 02 In The Presence of Frequency Hopping (Left) and Chirp (Right) Interference; With No Mitigation (Red), After Applying ANF (Blue) And WPD (Green).*

effects and some residual interference. The two techniques show relatively similar performance in the removal of a chirp signal. However, in the frequency hopping scenario (left), WPD-based mitigation (green) appears to better

recover the GPS signal resulting in higher C/N_0 than ANF (blue). Therefore, WPD appears to be the most suitable method for the removal of frequency hopping signals.

3. *Positioning*

The final contribution of this work is to provide an assessment of the impact of interference and its mitigation at the position level particularly focusing on the safety concerns. For this purpose, elevation, carrier to noise ratio (C/N_0) and hybrid (elevation and C/N_0) weighting models are applied for position estimation and also to estimate the protection level. The system performance is analyzed using the Stanford representation providing a quick and clear view of the KPIs including accuracy, availability and safety.

The positioning points in the Stanford diagram are distributed into several zones, each describing the state of the localization function. The significance of each zone is attributed to the capability to bound the true positioning error while respecting the application requirements defined by the alarm limit (AL). The points are classified into normal operation (white), misleading information – MI (pink and orange), system unavailable (yellow), and hazardous misleading information - HMI (red). Note, an Alarm limit (AL) of 30m is purposely chosen for this analysis which could vary depending on the application requirements.

Firstly, we present a reference case to show the positioning performance in the nominal conditions. This includes all the instances (epochs) before interference injection. In this manner, it generalizes the achievable performance with a specific configuration of the software receiver.

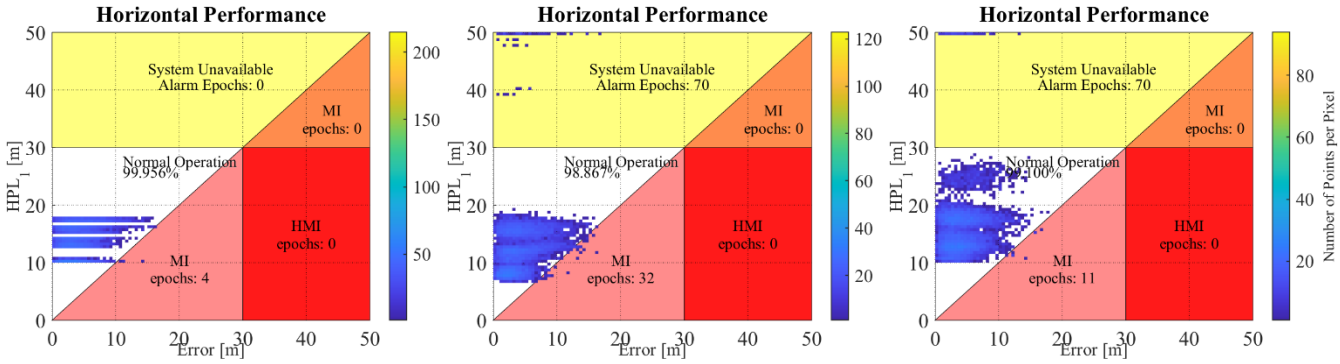

Figure 9 *Stanford Diagram Representing Performance in Nominal Condition Using Different Weighting Schemes; Elevation (Left), C/N_0 (Middle) And Hybrid (Right).*

In the absence of interference, no significant difference in the positioning accuracy is observed for each weighting model as seen in Figure 9. On average, the mean and the standard deviation of position error appear to be approximately 4.5m and 2.5m respectively. In a safety context, each model provides nearly 99% of normal operations ensuring the positioning integrity, however, with few misleading events. When C/N_0 based model is applied, some points are declared unavailable by the integrity monitoring criterion. As expected, the hybrid model tends to be the most conservative with higher PL values.

Figure 10 represents positioning performance in the presence of interference with no mitigation applied for the chirp and the frequency hopping scenario. We can clearly see that the nominal operation reduced significantly no matter the weighting model implemented. This highlights the importance of a mitigation process for the removal of the interference signal which when not mitigated raises safety concerns for the localization system and consequently of the entire system. Interference clearly shows an adverse impact on positioning accuracy represented by a higher concentration of points in HMI (> 50 m error). Moreover, the C/N_0 and hybrid model compared to the elevation-based weighting model in some way played a role in managing the effects of interference by increasing the protection level. This resulted in compensating some HMI with unavailability for system protection which is nevertheless enough to completely isolate positioning points affected by interference.

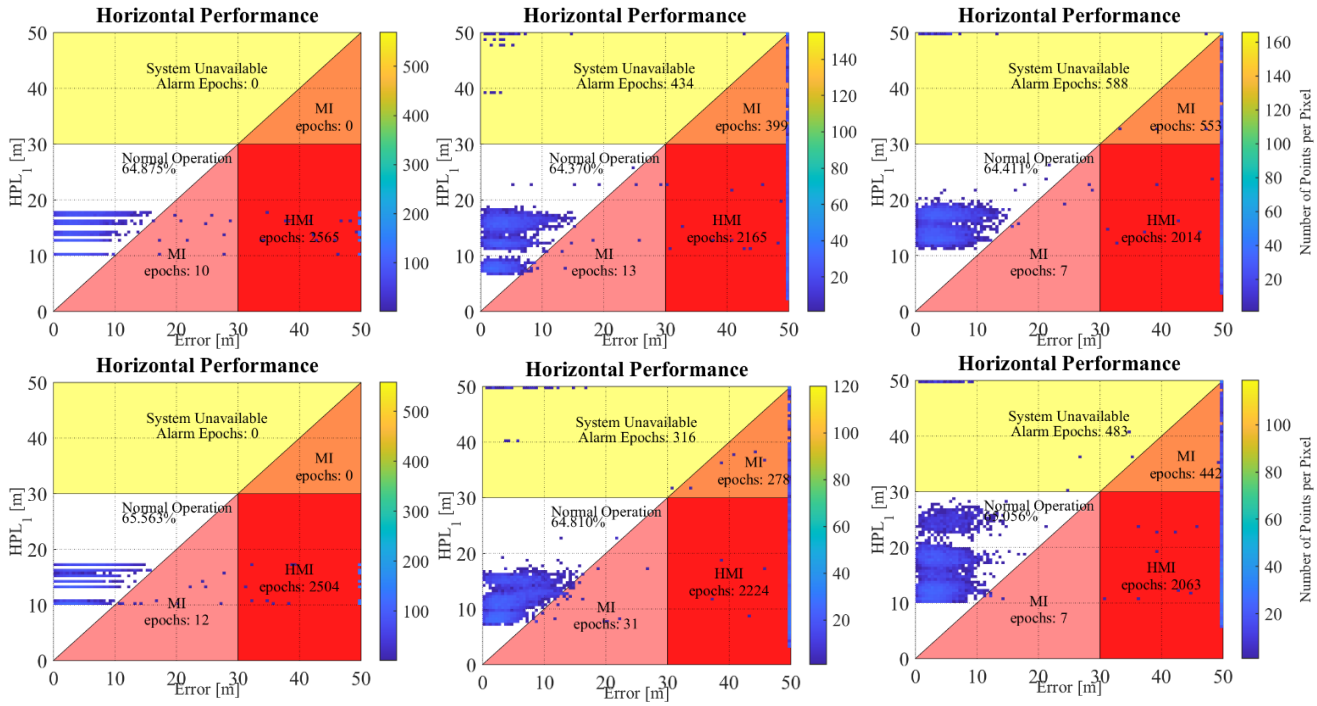

Figure 10 *Stanford Diagram Representing Performance in The Presence of Interference; Chirp (Upper Panel) And Frequency Hopping (Lower Panel) Prior To Mitigation, Using Weighting Schemes; Elevation (Left), C/N₀ (Middle) And Hybrid (Right)*

Figure 11 represents the positioning performance achieved after applying ANF (upper panel) and WPD (lower panel) techniques for the removal of the chirp signal. It can be seen that each mitigation technique significantly improves normal operations, however, they showed similar performance in combating the chirp signal. The elevation model appears to maximize the normal operation (white) to more than 96% but some points remain unbounded resulting in more MIs (pink). On the contrary, the C/N_0 and Hybrid model appears to be over-protective thus it brings some

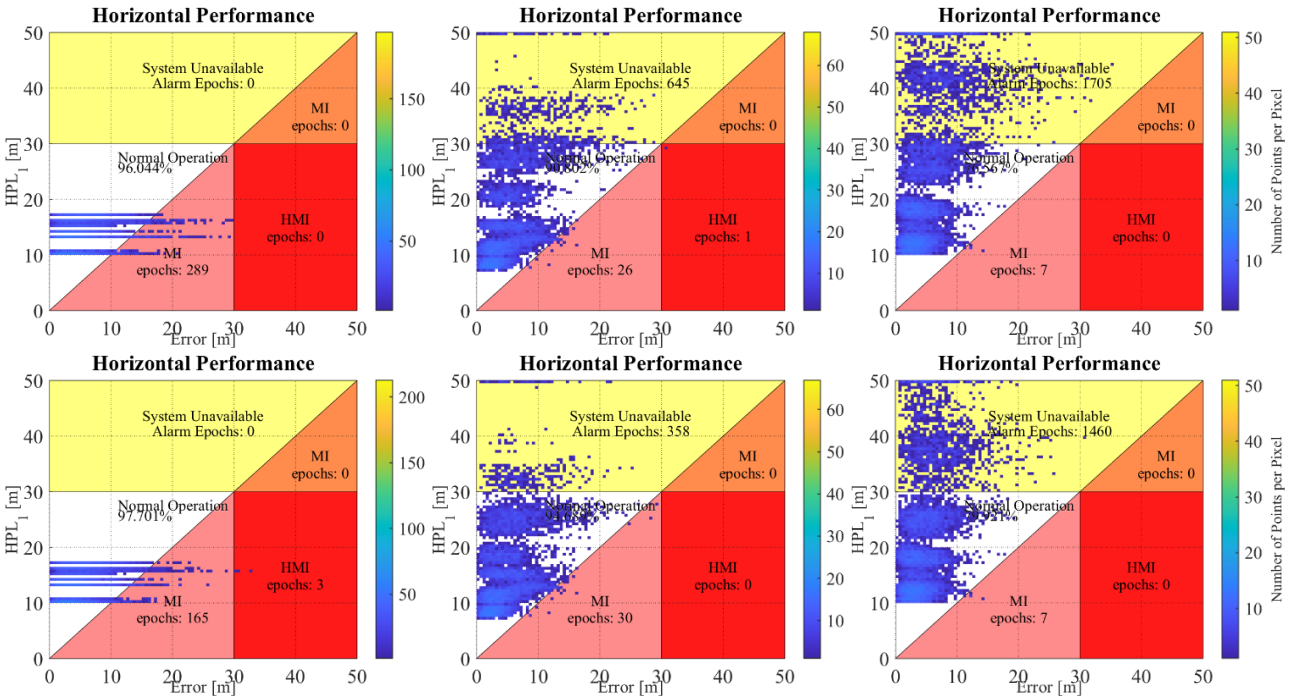

Figure 11 *Stanford Diagram Representing Performance After Mitigation of Chirp Signal by ANF (Upper Panel) And WPD (Lower Panel), Using Weighting Schemes; Elevation (Left), C/N₀ (Middle) And Hybrid (Right)*

additional undue unavailability (yellow) which is more the case in the hybrid model. The drop in C/N_0 (as seen in Figure 8) appears to be a probable cause of such overprotection since each measurement experiences similar behavior thus increasing the overall protection level.

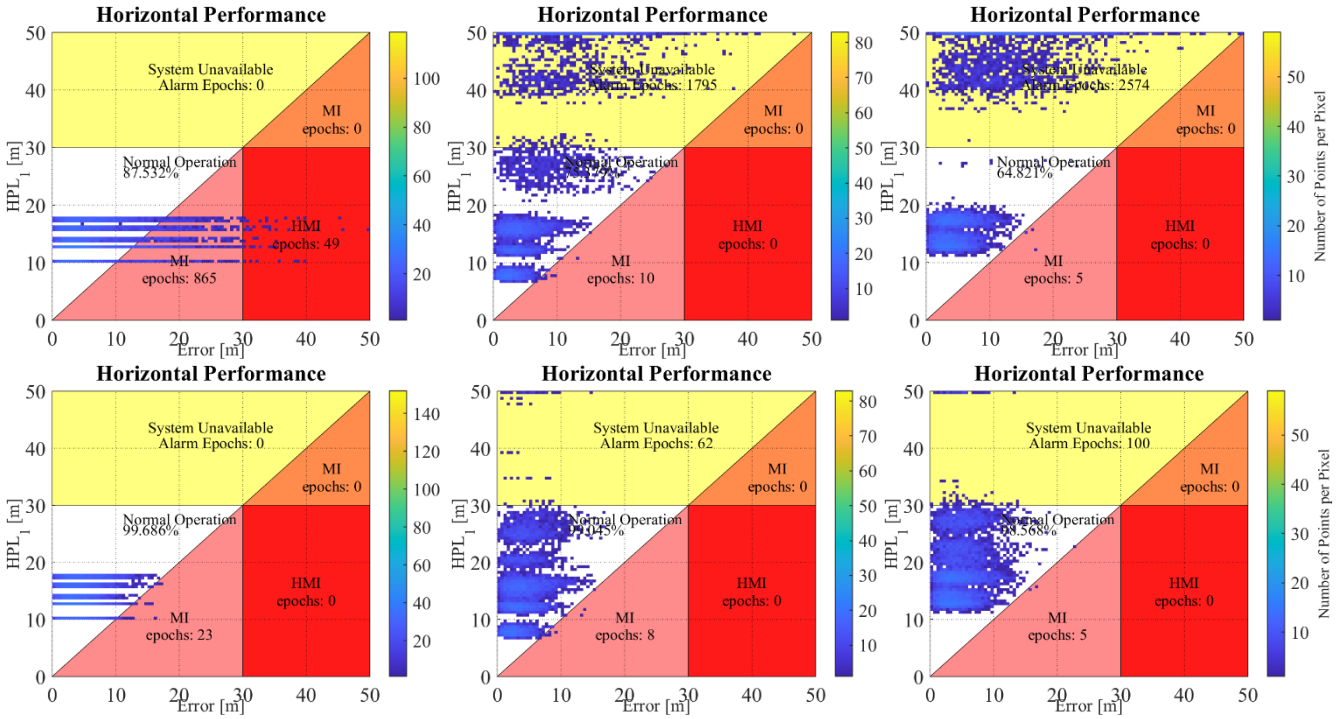

Figure 12 *Stanford Diagram Representing Performance After Mitigation of Frequency Hopping Signal by ANF (Upper Panel) And WPD (Lower Panel), Using Weighting Schemes; Elevation (Left), C/N_0 (Middle) And Hybrid (Right)*

Figure 12 presents the positioning performance after applying ANF (upper panel) for suppressing the frequency hopping signal. It can be seen that the effectiveness of ANF has reduced significantly in the frequency case compared to the previously presented chirp signal. Interference mitigation has resulted in a significant decrease in HMIs events however there remain some points with more than 30 m of positioning error. The elevation-based model still appears to be the most unsafe with 865 MIs (pink) and 49 HMIs (red) whereas C/N_0 and the hybrid model manage to remove the HMI events however resulting in higher system unavailability. It can also be seen that WPD-based mitigation outperformed ANF in the removal of the frequency hopping signal. It retrieved a similar performance as the reference scenario (as seen in Figure 9). It has significantly increased the nominal operations (white) and more importantly, it completely ensures system safety.

CONCLUSION

This paper reports an experimental analysis of interference mitigation with either ANF or WPD techniques. With this study, we contributed to address the impact of interference and the effectiveness of mitigation strategy from a safety (integrity) and user perspective. We presented three cases: 1) reference – without interference, 2) in the presence of interference but without any mitigation technique, and 3) after applying mitigation technique. For comparison analysis, we prepared two interference scenarios; linear chirp and frequency hopping. Furthermore, classical weighting schemes based on elevation, carrier to noise ratio (C/N_0) and hybrid (combination of elevation and C/N_0) model are used to estimate the position and the protection level.

The main conclusions can be summarized as follows. A detection and mitigation layer in the localization function is very essential to effectively remove the disturbances induced by the jamming signal. Indeed, as shown, an inadequate strategy can lead to hazardous consequences endangering the safety of the system eventually resulting in a fatal accident. However, interference mitigation at the signal level cannot guarantee to bring back the localization function to normal operation meeting the performance requirements. In most of the presented scenarios, mitigation significantly

reduced HMIs but with increasing unavailability, as a tradeoff to compromise availability for the system safety. This could be improved by introducing a complementary source of positioning to keep the system in nominal conditions.

The primary concern of an adaptive notch filter (ANF) is the appropriate selection of the filter parameters. It requires proper tuning that could vary depending on the characteristics of the jamming signal. Certainly, interference characterization could help in refining the choice of these parameters to improve mitigation performance and to retrieve the nominal situation. Additionally, the undue unavailability could also be reduced by the use of specific weighting calibration for the interference case.

WPD performed exceptionally well for the frequency hopping case as it nearly retrieved the same performance as in the nominal conditions. However, it could not provide similar performance for the removal of the chirp signal. Conceivably, changing wavelet function, filter length and (or) decomposition level could help in improving the performance against the chirp signal. This prospect needs to be investigated in future work.

ACKNOWLEDGEMENTS
The present work benefits from the financial support of the ANR French Research Agency within the project LOCSP No 2019-CE22-0011

REFERENCES

Anyaegbu, E., Brodin, G., Cooper, J., Aguado, E., & Boussakta, S. (2008). An integrated pulsed interference mitigation for GNSS receivers. *The Journal of Navigation*, *61*(2), 239.

Borio, D. (2016). Loop analysis of adaptive notch filters. *IET Signal Processing*, *10*(6), 659–669.

Borio, D., Camoriano, L., & Presti, L. Lo. (2008). Two-pole and multi-pole notch filters: a computationally effective solution for GNSS interference detection and mitigation. *IEEE Systems Journal*, *2*(1), 38–47.

Borio, D., Camoriano, L., Savasta, S., & Presti, L. Lo. (2008). Time-Frequency Excision for GNSS Applications. *IEEE Systems Journal*, *2*(1), 27–37. https://doi.org/10.1109/JSYST.2007.914914

Borio, D., & Cano, E. (2013). Optimal global navigation satellite system pulse blanking in the presence of signal quantisation. *IET Signal Processing*, *7*(5), 400–410.

Borio, D., & Gioia, C. (2021). GNSS interference mitigation: A measurement and position domain assessment. *Navigation, Journal of the Institute of Navigation*, *68*(1), 93–114. https://doi.org/10.1002/navi.391

Dovis, F. (2015). *GNSS Interference Threats and Countermeasures*. Artech House.

Dovis, F., Musumeci, L., & Samson, J. (2012). Performance comparison of transformed-domain techniques for pulsed interference mitigation. *Proceedings of the 25th International Technical Meeting of the Satellite Division of The Institute of Navigation (ION GNSS 2012)*, 3530–3541.

Fu, Z., Hornbostel, A., Hammesfahr, J., & Konovaltsev, A. (2003). Suppression of multipath and jamming signals by digital beamforming for GPS/Galileo applications. *GPS Solutions*, *6*(4), 257–264.

Gioia, C., & Borio, D. (2021). *Multi-layered Multi-constellation GNSS Interference Mitigation*. 1796–1808.

Groves, P. D., & Long, D. C. (2005). Combating GNSS interference with advanced inertial integration. *The Journal of Navigation*, *58*(3), 419.

Gupta, I. J., & Moore, T. D. (2003). Space-frequency adaptive processing (SFAP) for RFI mitigation in spread spectrum receivers. *IEEE Antennas and Propagation Society International Symposium. Digest. Held in Conjunction with: USNC/CNC/URSI North American Radio Sci. Meeting (Cat. No. 03CH37450)*, *4*, 172–175.

Hartinger, H., & Brunner, F. K. (1999). Variances of GPS Phase Observations: The SIGMA-ε Model. *GPS Solutions 1999 2:4*, *2*(4), 35–43. https://doi.org/10.1007/PL00012765

Kazim, S. A., Tmazirte, N. A., & Marais, J. (2021). On the impact of temporal variation on GNSS position error models. *ION 2021 International Technical Meeting Proceedings*, 728–737. https://doi.org/10.33012/2021.17863

Landry, R. J., Calmettes, V., & Bousquet, M. (1998). Impact of interference on a generic GPS receiver and assessment of mitigation techniques. *1998 IEEE 5th International Symposium on Spread Spectrum Techniques and Applications-Proceedings. Spread Technology to Africa (Cat. No. 98TH8333)*, *1*, 87–91.

Lashley, M., Bevly, D. M., & Hung, J. Y. (2009). Performance analysis of vector tracking algorithms for weak GPS signals in high dynamics. *IEEE Journal of Selected Topics in Signal Processing*, *3*(4), 661–673.

Musumeci, L., Curran, J. T., & Dovis, F. (2016). A Comparative Analysis of Adaptive Notch Filtering and Wavelet Mitigation against Jammers Interference. In *Navigation, Journal of the Institute of Navigation* (Vol. 63, Issue 4, pp. 533–550). https://doi.org/10.1002/navi.167

Musumeci, L., & Dovis, F. (2014). Use of the wavelet transform for interference detection and mitigation in global navigation satellite systems. *International Journal of Navigation and Observation*, *2014*. https://doi.org/10.1155/2014/262186

Musumeci, L., & Dovis, F. (2013). Performance assessment of wavelet based techniques in mitigating narrow-band interference. *2013 International Conference on Localization and GNSS (ICL-GNSS)*, 1–6.

Nunes, F. D., Margal, J. M. S., & Sousa, F. M. G. (2010). Low-complexity VDLL receiver for multi-GNSS constellations. *2010 5th ESA Workshop on Satellite Navigation Technologies and European Workshop on GNSS Signals and Signal Processing (NAVITEC)*, 1–8.

Qin, W., Gamba, M. T., Falletti, E., & Dovis, F. (2020). An Assessment of Impact of Adaptive Notch Filters for Interference Removal on the Signal Processing Stages of a GNSS Receiver. *IEEE Transactions on Aerospace and Electronic Systems*, *56*(5), 4067–4082. https://doi.org/10.1109/TAES.2020.2990148

Seo, B.-S., Kwi-Woo, P., & Chansik, P. (2019). Performance of Interference Mitigation with Different Wavelets in Global Positioning Systems. *Journal of Positioning, Navigation, and Timing*, *8*(4), 165–173.

Tay, S., & Marais, J. (2013). Weighting models for GPS Pseudorange observations for land transportation in urban canyons. *6th European Workshop on GNSS Signals and Signal Processing*.

Walter, T., & Enge, P. (1995). Weighted RAIM for Precision Approach. *In PROCEEDINGS OF ION GPS (1995) Institute of Navigation*, 1995–2004.